

**DECONVOLUTION OF GALILEO NIMS DAY-SIDE SPECTRA OF IO INTO THERMAL, SO<sub>2</sub>, AND NON-SO<sub>2</sub> COMPONENTS.** L. A. Soderblom<sup>1</sup>, K. J. Becker<sup>1</sup>, T. L. Becker<sup>1</sup>, R. W. Carlson<sup>2</sup>, A. G. Davies<sup>2</sup>, J. S. Kargel<sup>1</sup>, R. L. Kirk<sup>1</sup>, R. C. Lopes-Gautier<sup>2</sup>, W. D. Smythe<sup>2</sup>, and J. M. Torson<sup>1</sup>, <sup>1</sup>U. S. Geological Survey, 2255 N. Gemini Dr., Flagstaff, AZ 86001-1698; email: [lsoderblom@usgs.gov](mailto:lsoderblom@usgs.gov), <sup>2</sup>Jet Propulsion Laboratory, California Institute of Technology, 4800 Oak Grove Dr., Pasadena CA 91109-8099.

**Introduction:** Galileo NIMS (Near Infrared Mapping Spectrometer) spectra have been collected for both day-side and night-side Io hemispheres. The night-side data have been most readily analyzed to study thermal emission from Io's volcanic centers [1]. Analysis of the day-side data for the hot spots has been problematical owing to inseparability thermal emission and spectral reflectance and to interference of strong coherent-pattern noises. The latter effect arises from the following: NIMS uses 17 discrete detectors; each detector scans a section of the spectral range, accomplished by rotating a grating through discrete positions. As the field-of-view moves across high-contrast targets (e.g. volcanic hot spots) while the spectra are acquired, coherent patterns are introduced. NIMS spectral cubes are resampled using instrument pointing data reconstructed from spacecraft telemetry files to remove this effect and to re-register the spectra. Residual errors remain owing to uncertainties in the pointing data. The patterns can be estimated and removed using Fourier techniques operating on individual spectra. The analysis is complicated by several factors: 1) random noise spikes of a wide range of amplitude are present owing to the radiation environment---these must somehow be recognized and nulled out, in particular those of the same amplitude or larger than the coherent pattern noise, 2) in addition to nulls from removing spikes, sections of data are missing elsewhere in the spectra from various causes (saturated parts, inoperative detectors, downlink data losses, partial spectral sequences, etc.)---these nulled areas must be filled for the Fourier techniques to operate but filling them dilutes the strength of the coherent noise requiring iterative procedures, and 3) two separate coherent noise patterns, each varying in strength across the spectrum, exist in the Io spectra. The first two problems can be dealt with through iteration. The last problem arises because both thermal emission from volcanic hotspots (2-5  $\mu\text{m}$  region) and reflected sunlight are significant components of Io's spectra.

**Approach and Results:** The existence of these two coherent noise patterns can be taken to good advantage. The individual patterns can be extracted and then used to deconvolve individual spectra to estimate separately the contributions of the emitted and reflected components. This is important for study of thermal emission from the hotspots because it allows direct

estimation of the spectral form thermal flux without assumptions about either the nature of the emission (e.g. whether a single or composite blackbody) or about the spectral reflectance signature that is imbedded in the thermal-region spectrum. The approach is essential for studying the spectral reflectance of the hot-spot materials themselves in that it allows separation of the spectral reflectance from the strong thermal emission pattern that dominates the 2-5  $\mu\text{m}$  region. Fig. 1 shows results of this process for the central part

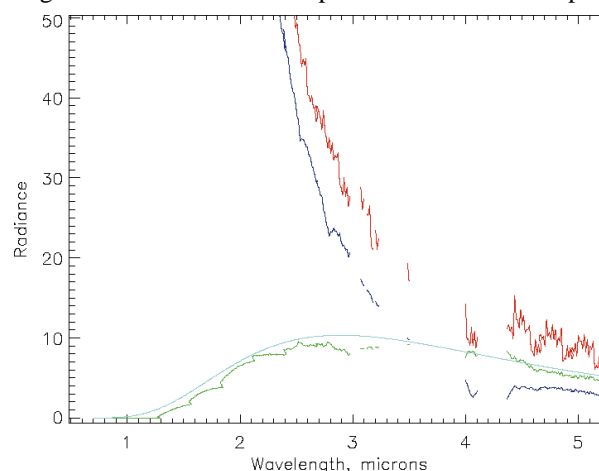


Figure 1 Deconvolution of NIMS spectrum of the central region of Pele on Io; all spectra are in radiance units (arbitrary scale). From top down: original spectrum (red), reflected component (blue), emitted component (green), 1000K blackbody (cyan)

of Pele. The blackbody form of the Pele emission was in no way a natural consequence of the deconvolution procedure---no assumption was made about the nature or functional form of the thermal component other than it was smooth on the scale of spectral ranges ( $\sim 0.2$ - $0.4 \mu\text{m}$ ) covered by individual detectors. The estimated 1000K blackbody emission is consistent with earlier analyses of NIMS dark-side spectra [1].

Once the two coherent patterns, random spikes, thermal, and reflected components have been estimated and deconvolved, the reflectance spectra can be averaged to search for new compositional signatures. A similar analysis was done earlier using this same day-side NIMS observation from orbit G2 by selecting spectra that were least noisy and least contaminated by thermal emission [2]. In that study Carlson and colleagues identified  $\sim 14$  features due to SO<sub>2</sub> of varying grain

size; a feature near 3.15  $\mu\text{m}$  previously reported and suggested as evidence of water in some form [3], and a broad absorption near 1  $\mu\text{m}$  of unknown origin. Fig. 2 shows a new average reflectance spectrum using the techniques described above for an equatorial belt in the

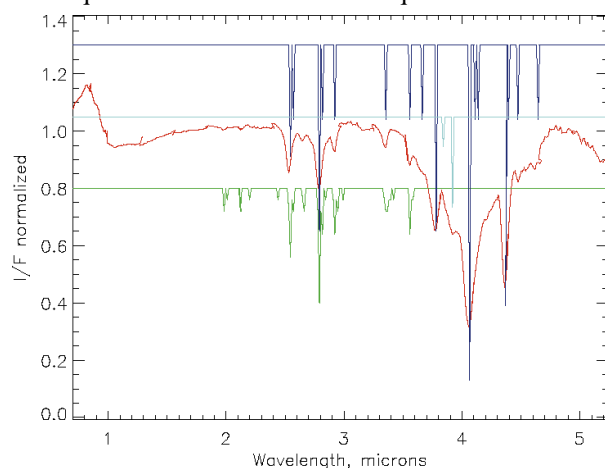


Figure 2 Deconvolved and averaged spectrum of broad equatorial band rich  $\text{SO}_2$  (red). For comparison absorption band centers for  $\text{SO}_2$  from laboratory data are shown: top (blue) Nash and Betts [4] frost spectra, middle (cyan) Nash and Betts [4] ice spectra, bottom (green) Schmitt et al [5] solid.

NIMS G2INHRSPEC01 observation that is richest in  $\text{SO}_2$ . Also plotted for reference are absorption band positions from  $\text{SO}_2$  laboratory spectra [4,5]. In addition to the features noted earlier [2] many weaker  $\text{SO}_2$  and other non- $\text{SO}_2$  features become apparent.

Our focus here, however, is in the 4.5-5.2  $\mu\text{m}$  region that has not been accessible until these new techniques were developed. Fig. 3 shows this spectral region for two separate regions (northern and southern mid-latitudes) and their average (middle curve). Care was taken that the north and south regions do not contain any of the same original data (through resampling of low-spatial-resolution spectra) so they are truly independent. Hence features that occur in both are real (i.e. not simply noise)---either relating to Io's surface or arising from NIMS calibration errors which is extremely unlikely remembering that each detector covers a broad wavelength range (the fly-back discontinuities in the spectra occur at wavelengths detector overlap---the data in fig. 3 are from detectors 15, 16, 17). Most notable to us are the absorptions with minima at 4.474 and 4.619  $\mu\text{m}$  although many other features are correlated between the north and south regions and are also likely to be real Io features (cf. 4.540, 4.580, 4.717, 4.783, 5.012, 5.144, 5.138  $\mu\text{m}$ ). Also shown in fig. 3 (as in the case of fig. 2) are known absorption band positions for  $\text{SO}_2$  [4]. The first (found by Nash and Betts at 4.476  $\mu\text{m}$ ) is a  $2\nu_1$  absorption of  $\text{SO}_2$  in the form of  $^{32}\text{S}^{18}\text{O}^{16}\text{O}$ . The second (found at 4.641  $\mu\text{m}$ )

is also thought by Nash and Betts to be  $\text{SO}_2$  but is unknown in terms of its vibrational characteristics. In any case we believe that the wavelength calibration of NIMS and the Nash and Betts spectra are so good as to preclude the absorption at 4.619  $\mu\text{m}$  in the Io spectra from being this  $\text{SO}_2$  band. The band wing on the slope between 4.65-4.70  $\mu\text{m}$  in the fig. 3 may well correspond this 4.641  $\mu\text{m}$   $\text{SO}_2$  laboratory feature. Our

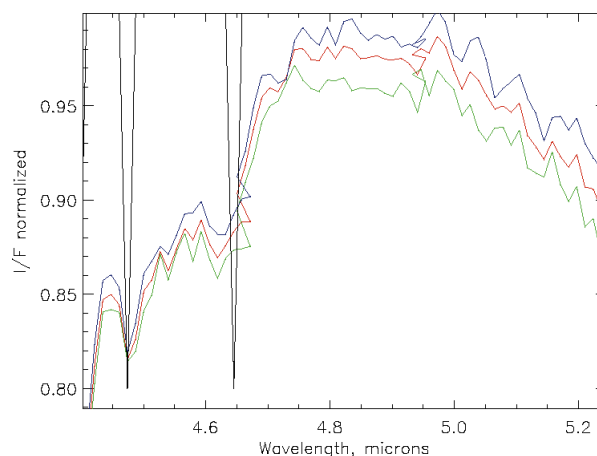


Figure 3 Averages of reflection spectra in the 4.5-5.2  $\mu\text{m}$  region for three areas on Io taken from NIMS observation G2INHRSPEC01 (central long.  $\sim 210^\circ\text{W}$ ). Upper curve (blue) northern mid-latitudes, bottom curve (green) southern mid-latitudes, middle curve (red) combination of the two. Two absorption band positions [4] are shown for  $\text{SO}_2$  frost.

analysis to assign composition to these features is just beginning. Cyanides and thiocyanates have a narrow deep feature in the  $4.62 \pm 0.05$   $\mu\text{m}$  region but these seem unlikely as no "Iogenic" C or N has been reported. Sulfur ( $\text{S}_8$ ) has a broad absorption near the  $4.65 \pm 0.01$   $\mu\text{m}$  but band width and position don't match well. Our tentative suggestion for the 4.619  $\mu\text{m}$  feature is some form of sulfate.

**References:** [1] Lopes-Gautier R. and members of the Galileo NIMS Team (1997) GRL, 24, 2439-2442. [2] Carlson R. W. and members of the Galileo NIMS Team (1997) GRL, 24, 2479-2442. [3] Salama F., Al-lamandola J., Witteborn F. C., Cruikshank D. P., Sandford S. A. and Bregman J. D. (1990) Icarus, 83, 66-82. [4] Nash D. B. and Betts B. H. (1995) Icarus, 117, 402-419. [5] Schmitt B., De Bergh C., Lellouch E., Maillard J-P, Barbe A. and Doute S. (1994) Icarus, 111, 70-105.